Synthesis of Mn_3O_4 Microflowers Anode Material for Lithium -ion Batteries with Enhanced Performance

ABSTRACT

It is important to prepare novel micro-nanostructures of Mn oxides for energy storage. A simple and versatile method for preparation of Mn_3O_4 microflowers associated with super-thin nanosheets is developed via a solvo-thermal approach, which are tested as a new high-capacity anode material for lithium-ion batteries. Mn_3O_4 microflowers~~It~~ shows better cycling performance than Mn_3O_4 nanoparticles. Research on this topic mainly sheds some light on the preparation of three-dimensional flower-like oxide hierarchical architectures with improved electrochemical performance for energy storage.

Keywords: Manganese oxide; Hierarchical architectures; Anode; Lithium-ion battery; Surfactant; Nanosheet.

1. INTRODUCTION

Rechargeable batteries with reversible and efficient electrochemical energy storage and conversion are urgent in various applications, such as portable electronic consumer devices, electric vehicles, and large-scale electricity storage in smart and intelligent grids as renewable and clean energy [1, 2]. Lithium-ion battery is one of the fascinating rechargeable batteries for high energy density coupled with a long life cycle and charge-discharge rate capability [3]. Studies have been conducted to develop low-cost, sustainable, renewable, safe, and high-energy density electrode materials for lithium-ion batteries. Considering environmental safety, researchers should prepare potential electrode materials for lithium-ion batteries through green chemistry based on simple and inexpensive procedures.

Manganese based anode materials are less toxic, abundant in natural resources [4]. Though Mn_3O_4 is isostructural with Co_3O_4, it has poor lithiation activity and electrically insulating, resulting in fast capacity decay as anode materials for lithium-ion batteries. Recently great progress has been achieved for Mn_3O_4 anode materials. The improved electrochemical properties turned true via the following methods. Mesoporous carbon, graphene, carbon nanotube and various carbon nanostructures were introduced to prepare carbon based Mn_3O_4 nano-composites. These composites showed better cycling stability and higher discharge capacity than bulk Mn_3O_4 for fast ion diffusion, good electronic conductivity, and skeleton supporting function [5-35]. People also designed various Mn_3O_4 nanostructures to improve the cycling performance of Mn_3O_4. In these Mn_3O_4 nanostructures, well-shaped nanostructure, pore, hollow structure and 3D array played an important role in the long cycling performance. Novel pongelike nanosized Mn_3O_4 exhibits a high initial reversible capacity of 869 mA h g^{-1} and significantly enhanced first coulomb efficiency with a stabilized reversible capacity of around 800 mA h g^{-1} after over 40 charge/discharge cycles [4]. Mn_3O_4 hollow microspheres demonstrate a good electrochemical performance, with a high reversible capacity of 646.9 mA h g^{-1} after 240 cycles at a current density of 200 mA h g^{-1}[36]~~].~~], ~~While~~ while pluorinated Mn_3O_4 nanospheres for lithium-ion batteries show poor cycling performances [37]. 3D porous Mn_3O_4 nanosheet arrays could be directly used as a binder-free and conductive-agent-free electrode to deliver ultrahigh electrochemical performance [38]. It is reported that the 3D pores and voids between the nanosheet arrays could provide rapid ion transfer channels, as well as accommodating the volumetric changes of Mn_3O_4 during the electrochemical cycling [38]. The ultrathin Mn_3O_4 nanosheets exhibit a high reversible capacity and stronger cycling stability for high surface area [39]. The well-shaped Mn_3O_4 tetragonal bipyramids with high-energy facets show a high initial discharge capacity. In addition, the anode displays a good fast rate performance and delivers a reversible capacity of 822.3 mA h g^{-1} (the theoretical capacity: 937 mA h g^{-1} at a current density of 0.2 C after 50 cycles [40]. The porous Mn_3O_4 nanorods can improve electrochemical reaction kinetics and favor the formation of Mn_3O_4 [41]. Mn_3O_4 nano-octahedra has a discharge capacity of 667.9 mA h g^{-1} after 1000 cycles at

1.0 A g^{-1} ascribed to the lower charge transfer resistance due to the exposed highly active {011} facets, which can facilitate the conversion reaction of Mn_3O_4 and Li owing to the alternating Mn and O atom layers, resulting in easy formation and decomposition of the amorphous Li_2O and the multi-electron reaction [42]. The hollow Mn_3O_4 spheres deliver a highly stable cycle performance with capacity retention of similar to 980 mA h g^{-1} for over 140 cycles at 200 mA g^{-1} and an excellent rate capability [43]. It can be seen that Mn_3O_4 with nanosheets, pore, high surface area and interconnected voids are apt to show high discharge capacity and long cycling stability. The 3D assembling Mn_3O_4 microflowers assembling with nanosheets are expected to show favorable electrochemical performances for the presence of voids among the nanosheet arrays. There are few reports on the research of Mn_3O_4 microflowers except Mn_3O_4-Fe_3O_4 and MnO- Mn_3O_4 nanoflowers. Mn_3O_4-Fe_3O_4 nanoflowers are simply fabricated through one step etching $Mn_5Fe_5Al_{90}$ ternary alloy, which exhibits higher performance as anode material for lithium ion batteries than that of pure Mn_3O_4 and Mn_3O_4 anodes for unique hierarchical flower-like structure and the synergistic effects between Mn_3O_4 and Mn_3O_4 [44]. A hierarchically porous MnO-Mn_3O_4 nano-flowers can be fabricated by dealloying Mn/Al alloys in aqueous NaOH solution in the presence of H_2O_2, and upon annealing, which has a capacity of 1018, 901 and 757 mA h g^{-1} with nearly 100% retention capacity after 100 cycles at 100, 200 and 500 mA g^{-1} [45]. Mn_3O_4 nanosheets associated with nanorods can be assembled to 3D flower-like Mn_3O_4 with hexadecyl trimethyl ammonium bromide (CTABr), urea and $MnSO_4$ as reagents, while they did not tested any properties, e.g. batteries [46].

In this study, a simple method was developed to prepare Mn_3O_4 microsflowers associated with nanosheets. These microflowers were synthesized in a N,N-dimethylformamide (DMF)–water solution with the aid of CTABr. When tested as an anode material for lithium-ion batteries, the Mn_3O_4 microflowers exhibited enhanced cycling stability than Mn_3O_4 nanoparticles.

2. MATERIAL AND METHODS / EXPERIMENTAL DETAILS / METHODOLOGY (ARIAL, BOLD, 11 FONT, LEFT ALIGNED, CAPS)

All chemicals are commercially available. The preparation was performed via a solvothermal method in a DMF-water mixed solvent. In a typical procedure, 1 mmol manganese acetate tetrahydrate and 0.5 g hexadecyl trimethyl ammonium bromide (CTABr) were added to a 5 ml DMF- 25 ml water solution and stirred at room temperature for 2 hours. After that, the mixture was transferred to a 50-ml Teflon-lined stainless autoclave, sealed, kept at 200 ^{O}C for 24 hours, cooled to room temperature, washed with absolute alcohol and dried at 70 ^{O}C for 12 hours (marked with DT-1). Sample DT-2 was prepared without CTABr under the identical condition. While Sample DT-3 was prepared with 30 ml water in the absence of CTABr.

The morphological characteristics of the as-synthesized materials were observed with a Hitachi S-4800 field emission scanning electron microscope (SEM). X-ray diffraction (XRD) patterns were recorded on a diffract meter (Co Kα, Analytical, and Pert). Cyclic voltammetry (CV) experiments were performed with a Chi660c electrochemical workstation at a scan rate of 1 mV S^{-1}. A Land CT2001A battery tester was used to measure the electrode activities at room temperature.

The as-synthesized samples were tested as anode materials for lithium-ion batteries. The composite of negative electrode material was consisted of the active material, a conductive material (super-pure carbon) and binder polyvinylidene difluoride (PVDF) in a weight ratio of 7/2/1. The Li metal was used as the counter electrode. The cells were charged and discharged between a 0.05 - 3.0 V voltage limit.

3. RESULTS AND DISCUSSION

Three samples were obtained by adjusting synthesis parameters. Both DMF and CTABr play an important role in the formation of different morphologies. When water was used as the solvent in the absence of CTABr, the sample appears as monodispersed nanoparticles between 30 and 150 nm in Fig. 1a,b. While DMF was added, thin microplatelets were obtained, as shown in Fig. 1c, d. The length and width of microplatelets can be up to several μm. There are also some thin nanobelts. Some microflowers composed of superimposed thin and wide nanosheets were prepared with CTABr in the DMF-H_2O mixed solvent in Fig. 1e, f. Certain microflower is several μm in size.

X-ray diffraction was performed to identify the structure of the three samples. It can be seen that CTABr plays an important role in the crystallization of products. The diffraction peaks of the sample prepared with DMF, water and CTABr has the highest intensity than samples prepared with water, CTABr and DMF in Fig. 2. The diffraction peaks can be ascribed to Mn_3O_4 in Fig. 2a (JCPDS 89-4837). The other samples can also be ascribed to Mn_3O_4 in Fig. 2b,c , respectively. All the Mn_3O_4 here are lack of the peak of (101), which means that the is not the high-energy {101} plane.

The electrochemical performance of Mn_3O_4 nanoparticles and microflowers was evaluated as anode materials for lithium-ion batteries (Fig. 3). Fig. 3a shows the 1st and 2nd charge–discharge profiles of Mn_3O_4 microflowers at a current density of 240 mA g^{-1} (Sample T-72). A long discharge platform is observed at 0.5 V in the first discharge curve, but this platform disappears in the succeeding discharge curves. The Mn_3O_4 microflowers-based composite electrode delivers an initial discharge capacity of 1496 mA h g^{-1}. However, the 1st discharge profiles of Mn_3O_4 nanoparticles show four discharge platforms at 0.33, 0.44, 0.92 and 1.3 V, implying that a multi-step conversion reaction takes place. A new platform at 0.7 V appears in the succeeding discharge curves. The Mn_3O_4 nanoparticles-based composite electrode delivers an initial discharge capacity of 1280 mA h g^{-1}. It can be seen that Mn_3O_4 without high-energy {101} plane can also have a very high initial discharge capacity. It can also be found that Mn_3O_4 nanoparticles have a steeper charge curve than Mn_3O_4 microflowers between 1.4 and 3.0 V implying that a severe polarization takes place in the Mn_3O_4 nanoparticles-based composite electrode.

We also performed the dQ/dV~V curves obtained from the 1st and 2nd charge-discharge curves of Mn_3O_4 nanoparticles and microflowers in Fig. 4. In the first charge-discharge cycle of Mn_3O_4 nanoparticles, four reduction peaks are centered at 0.33, 0.45, 0.90 and 1.3 V, and the oxidation peak is at 1.24 V in Fig. 4a. In the first charge-discharge cycle of Mn_3O_4 microflowers, the reduction and oxidation peaks are centered at 0.33 and 1.28 V in Fig. 4b, respectively. In the second charge-discharge cycle of Mn_3O_4 nanoparticles, two reduction peaks are centered at 0.45 and 0.52 V, and the oxidation peak is at 1.24 V in Fig. 5b. In the second charge-discharge cycle of Mn_3O_4 microflowers, the reduction and oxidation peaks are centered at 0.54 and 1.25 V in Fig. 2, respectively. The reduction peaks in the range of 1.3-0.4 V was ascribed to reduction from Mn(III) to Mn(II), and the 0.4-0.1 V range reflected the reduction from Mn(II) to Mn(0) [47,48]. The difference of first discharge curve between Mn_3O_4 microflowers and nanoparticles is because Mn_3O_4 microflowers only undergoes the reduction from Mn(II) to Mn(0). While Mn_3O_4 nanoparticles undergo reductions from Mn(III) to Mn(II) to Mn(0). In the second discharge process, In the second discharge, the contribution to discharge capacity is mainly ascribed to the reduction around 0.5 V. The Li+ charge reaction: is Mn_3O_4 + 8Li+ + 8e- to 3Mn(0) + 8Li_2O [49]. Compared to Mn_3O_4 nanoparticles, Mn_3O_4 microflowers does not undergo reduction from Mn(III) to Mn(II) and reduce polarization.

Fig.6 is the cycling performance testes at current densities of 240 and 480 mA g^{-1}. The Mn_3O_4 microflowers-based composite electrode delivers a second discharge capacity of 870.2 and 714.8 mA h g^{-1} in Fig. 6a,b, respectively . A reversible capacity of 392.8 and 358.5 mA h g^{-1} is retained after 20 cycles. The Mn_3O_4 nanoparticles-based composite electrode show lower discharge capacity and worse cycling stability at current densities of 240 and 480 mA g^{-1} in Fig. 6c,d. It delivers a second discharge capacity of 332.8 and 156.5 mA h g^{-1}, respectively. The final discharge capacity is even low to 131.3 and 53.8 mA h g^{-1}. The fast capacity decay of Mn_3O_4 nanoparticles is due to the reduction from Mn(III) to Mn(II). The improved electrochemical performance of Mn_3O_4 microflowers is due to reduce the activity of Mn_3O_4, avoid the complicated reduction from Mn(III) to Mn(II) and reduce polarization. We have focused on the research of flower-like rutile TiO_2 and ammonium vanadium bronze. We found that the effect of flower-like nanostructures on the reaction kinetics of the electrode are ascribe to the changes the total impedance and electron transfer resistance [50, 51].The improved performance of Mn_3O_4 micro-flowers is also ascribed to improve the transferring of electron.

Comment [M1]: Text mentions Fig 5.b but Fig 5.a has not been mentioned.

Comment [M2]:

Comment [M3R2]: Repeated.

Comment [M4]: Seems to be an equation reaction. If this is the case, normallly an arrow (→) is used to separate reagents from products of reaction.

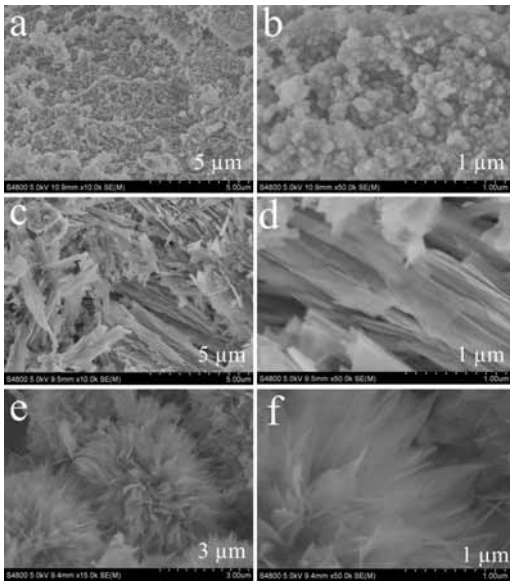

Fig. 1. SEM images of samples with (a, b) water, (c, d) water and DMF, and (e, f) water, DMF and CTABr

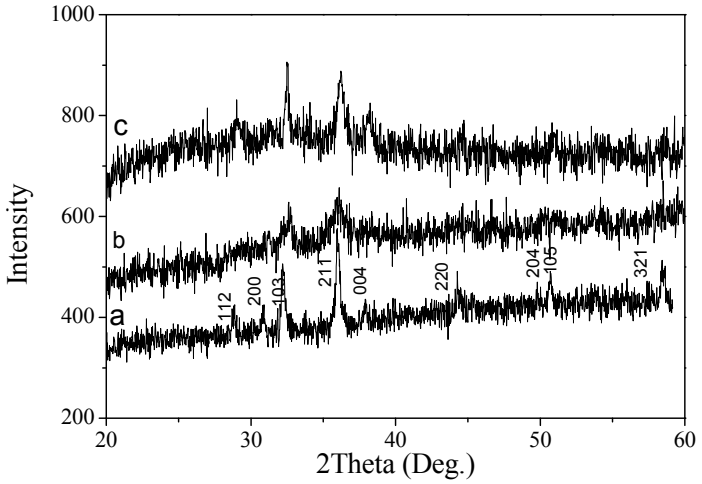

Fig. 2. Wide angle XRD patterns of samples with (a) water, DMF and CTABr, (b) water and DMF, and (c) water

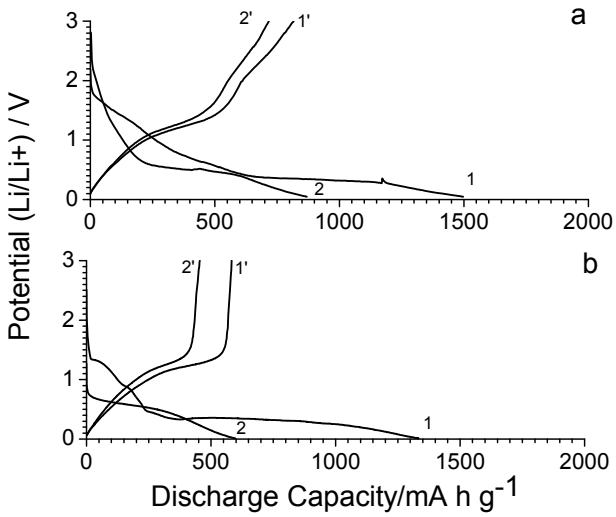

Fig. 3. The first and second charge–discharge profiles at a current density of 240 mA g^{-1} of (a) Mn_3O_4 microflowers and (b) Mn_3O_4 nanoparticles

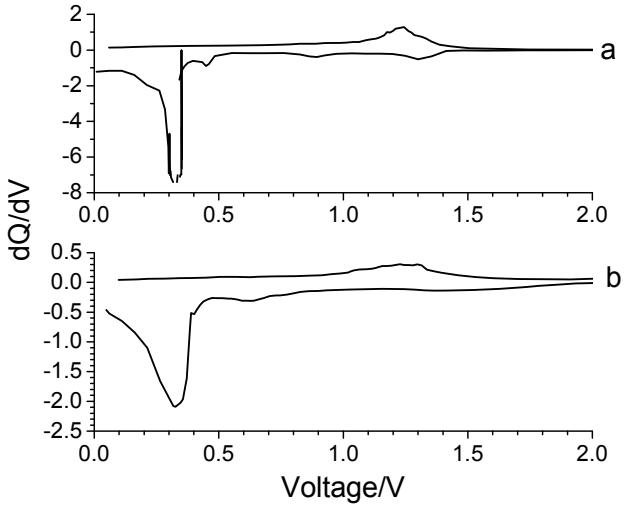

Fig. 4. The dQ/dV~cueve derived the first charge–discharge profiles of (a) Mn_3O_4 nanoparticles (b) Mn_3O_4microflowers

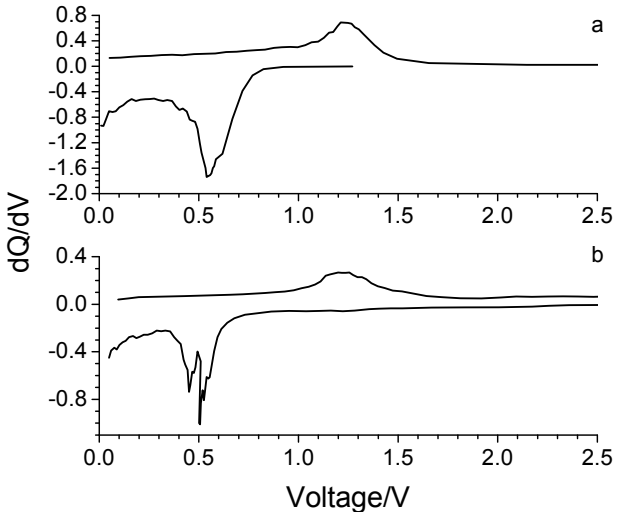

Fig. 5. The dQ/dV~cueve derived the second charge–discharge profiles of (a) Mn_3O_4 microflowers (b) Mn_3O_4 nanoparticles

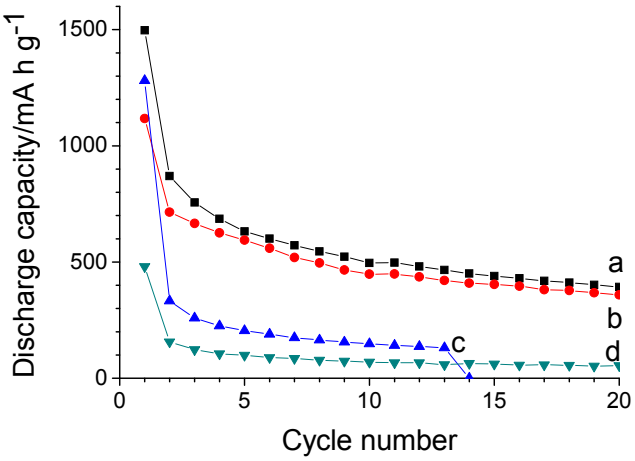

Fig. 6. The cyclic performance tested at current densities of 240 and 480 mA g^{-1} of (a, b) Mn_3O_4 microflowers, and (c, d) Mn_3O_4 nanoparticles

4. CONCLUSION

In summary, Mn_3O_4 microflowers associated with super-thin nanosheets were prepared by using a solvo-thermal method with the aid of surfactant CTABr. The Mn_3O_4 microflowers exhibit better cycling stability and higher discharge capacity than Mn_3O_4 nanoparticles as anode materials for lithium-ion batteries due to reduce the activity of Mn_3O_4, avoid the complicated reduction from Mn(III) to Mn(II) and reduce polarization. This simple method may also be used to fabricate other anode materials for lithium-ion batteries with improved electrochemical performance.

Comment [M5]: Conclusions should explore more the results obtained to really show the good work done by the author. A language review would make paper more clear and improve its quality.

REFERENCES

1. Cheng FY, Liang J, Tao ZL, Chen J. Functional materials for rechargeable batteries. Adv Mater. 2012;23:1695-1715.
2. Fei HL, Liu X, Li ZW. Hollow cobalt coordination polymer microspheres: a promising anode material for lithium-ion batteries with high performance. Chem Eng J. 2015;281:453-458.
3. Tarascon JM. Key challenges in future Li-battery research. Phil. Trans. R. Soc. A., 2010;368:3227-3241.
4. Gao J, Lowe MA, Abruña HD, Spongelike nanosized Mn_3O_4 as a high-capacity anode material for rechargeable lithium batteries. Chem Mater. 2011;23:3223-3227.
5. Zhang LP, Li GS, Fan JM, Li BY. In situ synthesis of Mn_3O_4 nanoparticles on hollow carbon nanofiber as high-performance lithium ion battery anode. Chem. 2018;DOI:10.1002/chem.201801196.
6. Guo LG, Ding Y, Qin CQ et al, Anchoring Mn_3O_4 nanoparticles onto nitrogen-doped porous carbon spheres derived from carboxymethyl chitosan as superior anodes for lithium-ion batteries. J Alloy Cmpd. 2018;735:209-217.
7. Song NJ, Ma CL. A green synthesis of Mn_3O_4 /graphene nanocomposite as anode material for lithium-ion batteries. Int J Electrochem Sci. 2018;13:452-460.
8. Wu LL, Zhao DL, Cheng XW, Ding ZW, Hu T, Meng S. Nanorod Mn_3O_4 anchored on graphene nanosheet as anode of lithium ion batteries with enhanced reversible capacity and cyclic performance. J Alloy Cmpd. 2018;728:383-390.
9. Li Z, Tang B, Mn_3O_4/nitrogen-doped porous carbon fiber hybrids involving multiple covalent interactions and open voids as flexible anodes for lithium-ion batteries. Green Chem. 2017;19:5862-5873.
10. Liu BB, Qi L, Ye JJ, Wang JQ, Xu CX. Facile fabrication of graphene-encapsulated Mn_3O_4 octahedra cross-linked with a silver network as a high-capacity anode material for lithium ion batteries, New J Chem. 2017;41:13454-13461.
11. Peng HJ, Hao GX, Chu ZH, Lin J, Lin XM, Cai YP. Mesoporous Mn_3O_4/C microspheres fabricated from MOF template as advanced lithium-ion battery anode. Crys Growth & Des. 2017;11:5881-5886.
12. Lv KK, Zhang YH, Zhang DY, Ren WW, Sun L. Mn_3O_4 nanoparticles embedded in 3D reduced graphene oxide network as anode for high-performance lithium ion batteries. J Mater Sci-Mater. El., 2017;28:14919-14927.
13. Pramanik A, Maiti S, Sreemany M, Mahanty S. Rock-salt-templated Mn_3O_4 nanoparticles encapsulated in a mesoporous 2D carbon matrix: a high rate 2 V anode for lithium-ion batteries with extraordinary cycling stability. Chemistryselect, 2017;2:854-7864.
14. Zhang R, Wang D, Qin LC, $MnCO_3$/ Mn_3O_4/reduced graphene oxide ternary anode materials for lithium-ion batteries: facile green synthesis and enhanced electrochemical performance. J Mater Chem A, 2017;5:17001-17011.
15. Zhuang YC, Ma Z, Deng YM, Song XN, Zuo XX, Xiao X, Nan JM. Sandwich-like Mn_3O_4/carbon nanofragment composites with a higher capacity than commercial graphite and hierarchical voltage plateaus for lithium ion batteries. Electrochim Acta. 2017;440-447.
16. Yang ZL, Lu DL, Zhao RR, Gao AM, Chen HY. Synthesis of a novel structured Mn_3O_4@C composite and its performance as anode for lithium ion battery. Mater Lett. 2017;198:97-100.
17. Cui X, Wang YQ, Xu QY, Sun P, Wang XZ , Wei T, Sun YM. Carbon nanotube entangled Mn_3O_4 octahedron as anode materials for lithium-ion batteries. Nanotech. 2017;28:255402.
18. Chen JY, Wu XF, Gong Y, Wang PF, Li WH, Tan QQ, Chen YF. Synthesis of Mn_3O_4/N-doped graphene hybrid and its improved electrochemical performance forlithium-ion batteries. Ceram Int. 2017;43:4655-4662.
19. Gangaraju D, Sridhar V, Lee I, Park H. Graphene - carbon nanotube - Mn_3O_4 mesoporous nano-alloys as high capacity anodes for lithium-ion batteries. J Alloy Cmpd. 2017;699:106-111.
20. Seong CY, Park SK, Bae Y, Yooa S, Piao Y. An acid-treated reduced graphene oxide/ Mn_3O_4 nanorod nanocomposite as an enhanced anode material for lithium ion batteries. Rsc Adv. 2017;7:37502-37507.
21. Park I, Kim T, Park H, Mun M, Shim SE, Baeck SH. Preparation and electrochemical properties of Pt-Ru/ Mn_3O_4/C bifunctional catalysts for lithium-air secondary battery. J Nanosci. Nanotechno. 2016;16:10453-10458.

22. Zhang Y, Yue KQ, Zhao HS, Wu Y, Duan LF, Wang KL. Bovine serum albumin assisted synthesis of Fe_3O_4@C@ Mn_3O_4 multilayer core-shell porous spheres as anodes for lithium ion battery. Chem Eng J. 2016;291:238-243.
23. Park SK, Seong CY, Yoo S, Piao Y. Porous Mn_3O_4 nanorod/reduced graphene oxide hybrid paper as a flexible and binder-free anode material for lithium ion battery.Energy, 2016;99:266-273.
24. Alfaruqi MH, Gim J, Kim S, Song J, Duong PT, Jo J, Baboo JP, Xiu Z, Mathew V, Kim J. One-step pyro-synthesis of a nanostructured Mn_3O_4/C electrode with long cycle stability for rechargeable lithium-ion batteries. Chem-A Eur J. 2016; 22:2039-2045.
25. Bhimanapati G, Yang RG, Robinson JA, Wang Q. Effect of Mn_3O_4 nanoparticle composition and distribution on graphene as a potential hybrid anode material for lithium-ion batteries. Rsc Adv. 2016;6:33022-33030.
26. Jing MJ, Wang JF, Hou HS, Yang YC, Zhang Y, Pan CC, Chen J, Zhu YR, Ji XB. Carbon quantum dot coated Mn_3O_4 with enhanced performances for lithium-ion batteries. J Mater Chem A. 2015;3:16824-16830.
27. Ren YR, Wang JW, Huang XB, Yang B, Ding JN. One step hydrothermal synthesis of Mn_3O_4/graphene composites with great electrochemical properties for lithium-ion batteries. Rsc Adv. 2015;5:59208-59217.
28. Yue HW, Li F, Yang ZB, Li XW, Lin SM, He DY. Facile preparation of Mn_3O_4-coated carbon nanofibers on copper foam as a high-capacity and long-life anode for lithium-ion batteries. J Mater Chem A. 2014;2:17352-17358.
29. Luo S, Wu HC, Wu Y, Jiang KL, Wang JP, Fan SS. Mn_3O_4 nanoparticles anchored on continuous carbon nanotube network as superior anodes forlithium ion batteries. J Power Sources, 2014;249:463-469.
30. Park SK, Jin A, Yu SH, Ha J, Jang B, Bong S, Woo S, Sung YE, Piao Y. In situ hydrothermal synthesis of Mn_3O_4 nanoparticles on nitrogen-doped graphene as high-performance anode materials for lithium ion batteries. Electrochim Acta, 2014;120:452-459.
31. Luo YQ, Fan SS, Hao NY, Zhong SL, Liu WC. An ultrasound-assisted approach to synthesize Mn_3O_4/RGO hybrids with high capability forlithium ion batteries. Dalton T. 2014;43:15317-15320.
32. Lavoie N, Malenfant PRL, Courtel FM, Abu-Lebdeh Y, Davidson IJ, High gravimetric capacity and long cycle life in Mn_3O_4/graphene platelet/LiCMC compositelithium-ion battery anodes. J Power Sources 2012;213:249-254.
33. Wang ZH, Yuan LX, Shao QG, Huang F, Huang YH. Mn_3O_4 nanocrystals anchored on multi-walled carbon nanotubes as high-performance anode materials for lithium-ion batteries. Mater Lett. 2012;80:110-113.
34. Wang CB, Yin LW, Xiang D, Qi YX. Uniform carbon layer coated Mn_3O_4 nanorod anodes with improved reversible capacity and cyclic stability for lithium ion batteries. ACS Appl Mater Inter. 2012;4:1636-1642.
35. Li ZQ, Liu NN, Wang XK, Wang CB, Qi YX, Yin LW. Three-dimensional nanohybrids of Mn_3O_4/ordered mesoporous carbons for high performance anode materials for lithium-ion batteries. J Mater Chem. 2012;22:16640-16648.
36. Palaniyandy N, Nkosi FP, Raju K, Ozoemena KI. Fluorinated Mn_3O_4 nanospheres for lithium-ion batteries: Low-cost synthesis with enhanced capacity, cyclability and charge-transport. Mater Chem Phys. 2018;209:65-75.
37. Jiang Z, Huang KH, Yang D, Wang S, Zhong H, Jiang CW. Facile preparation of Mn_3O_4 hollow microspheres via reduction of pentachloropyridine and their performance in lithium-ion batteries. RSC Adv. 2017;3:8264-8271.
38. Fan XY, Cui Y, Liu P, Gou L, Xu L, Li DL. Electrochemical construction of three-dimensional porous Mn_3O_4 nanosheet arrays as an anode for the lithium ion battery. Phys Chem Chem Phys. 2016;18:22224-22234.
39. Zhen MM, Zhang Z, Ren QT, Liu L. Room-temperature synthesis of ultrathin Mn_3O_4 nanosheets as anode materials for lithium-ion batteries. Mater Lett. 2016;177:21-24.
40. Li TT, Guo CL, Sun B, Li T, Li YG, Hou LF, Wei YH. Well-shaped Mn_3O_4 tetragonal bipyramids with good performance for lithium ion batteries. J Mater Chem A. 2015;3:7248-7254.
41. Bai ZC, Zhang XY, Zhang YW, Guo CL, Tang B. Facile synthesis of mesoporous Mn_3O_4 nanorods as a promising anode material for high performanceLithium-ion batteries. J Mater Chem A. 2014;2:16755-16760.
42. Huang SZ, Jin J, Cai Y, Li Y, Tan HY, Wang HE, Tendeloo GV, Su BL. Engineering single crystalline Mn_3O_4 nano-octahedra with exposed highly active {011} facets for high performance lithium ion batteries. Nanoscale, 2014;6 : 6819-6827.

43. Jian GQ, Xu YH, Lai LC, Wang CS, Zachariah MR. Mn_3O_4 hollow spheres for lithium-ion batteries with high rate and capacity. J Mater Chem A. 2014;2:4627-4632.
44. Zhao DY, Hao Q, Xu CX, Facile fabrication of composited Mn_3O_4/Fe_3O_4 nanoflowers with high electrochemical performance as anode material for lithium ion batteries. Electrochim Acta, 2015;180:493-500.
45. Wang JZ, Du N, Wu H, Zhang H, Yu JX, Yang DR, Order-aligned Mn_3O_4 nanostructures as super high-rate electrodes for rechargeable lithium-ion batteries. J. Power Sources, 2013;222:32-37.
46. Wang M, Cheng LM, Li QB, Chen ZW, Wang SL.Two-dimensional nanosheets associated with one-dimensional single-crystalline nanorods self-assembled into three-dimensional flower-like Mn_3O_4 hierarchical architectures. Phys Chem Chem Phys. 2014;39:21742-21746.
47. Pasero D, Reeves N, West AR, Co-doped Mn_3O_4: a possible anode material for lithium batteries. J Power Sources. 2005;141:156-158.
48. Wang HL, Cui LF, Yang Y, Casalongue HS, Robinson JT, Liang YY, Cui Y, Dai HJ. Mn_3O_4-graphene hybrid as a high-capacity anode material for lithium ion batteries. J Am Chem Soc. 2010;132:13978-13980.
49. Wu Z, Ren W, Wen L, Gao L, Zhao J, Chen Z, Zhou G. Li F, Cheng H. Graphene anchored with Co_3O_4 nanoparticles as anode of lithium ion batteries with enhanced reversible capacity and cyclic performance. ACS Nano, 2010;4:3187-3194.
50. Fei HL, Wei MD. Facile synthesis of hierarchical nanostructured rutile titania for lithium-ion battery. Electrochim Acta, 2011;56:6997-7004.
51. Fei HL, Li H, Li ZW, Feng WJ, Liu X, Wei MD. Facile synthesis of graphite nitrate-like ammonium vanadium bronzes and their graphene composites for sodium-ion battery cathodes. Dalton Trans, 2014; 43:16522-16527.